Available online at www.sciencedirect.com
SCIENCE DIRECT®
Chemical Physics Letters 400 (2004) 430–435
CHEMICAL PHYSICS LETTERS
www.elsevier.com/locate/cplett

Symmetry of electron diffraction from single-walled carbon nanotubes

Zejian Liu [a], Lu-Chang Qin [a,b,*]

[a] Department of Physics and Astronomy, University of North Carolina at Chapel Hill, CB #3255, Chapel Hill, NC 27599-3255, USA
[b] Curriculum in Applied and Materials Sciences, University of North Carolina at Chapel Hill, CB #3255, Chapel Hill, NC 27599-3255, USA

Received 6 October 2004; in final form 6 October 2004
Available online 18 November 2004

Abstract

We show that, even when the atomic structure of a single-walled carbon nanotube does not have mirror symmetry perpendicular to the tubule axis, the electron diffraction patterns of the single-walled carbon nanotube always possess 2mm symmetry. We have also analyzed the contributions of higher order Bessel functions to the intensity distribution on the layer lines and found that (a) their contributions are negligible and (b) they would not affect the symmetry of the diffraction pattern. Both experimental and simulated electron diffraction patterns of a single-walled carbon nanotube of indices (14, 9) are presented to illustrate the 2mm symmetry and to corroborate the theoretical analysis.

1. Introduction

Electron diffraction is a very powerful technique for determining the atomic structure (both diameter and helicity) of carbon nanotubes [1–9]. Due to the finite size of carbon nanotubes in the radial directions, the intensity distribution of the electron diffraction pattern from a carbon nanotube deviates noticeably from that of graphene which gives rise to hexagonal symmetry. The electron diffraction intensities elongate perpendicular to the tubule axis and form a set of layer lines normal to the tubule axis. The elongated intensity distribution stipulates that the electron diffraction pattern from carbon nanotubes loses hexagonal symmetry. But it has been observed experimentally that the electron diffraction pattern of a single-walled carbon nanotube showed 2mm symmetry [2]. This conclusion has recently been challenged in an analysis based on the analytic solutions to the scattering amplitude of electron scattering [10,11], where the authors argue that the 2mm symmetry usually does not exist in the electron diffraction patterns of a single-walled carbon nanotube unless the atomic structure of the nanotube satisfies some special conditions, i.e., the crystallographic indices (u, v) are all even [12]. The analytic approach makes use of the additions of the Bessel functions that appear in the expression of the scattering intensities.

Since the atomic structure of a single-walled carbon nanotube generally does not have mirror symmetry perpendicular to the tubule axis, it is not obvious to deduce that its electron diffraction pattern should have 2mm symmetry from consideration of geometric symmetry alone. Experimentally, we have examined a large number of carbon nanotubes of various atomic structures, and all the diffraction patterns show 2mm symmetry [13]. In this Letter, we employ analytic expressions, experimental observations, and numerical simulations of electron diffraction patterns from single-walled carbon nanotubes to demonstrate that 2mm symmetry is always present in the intensity distribution. In addition,

* Corresponding author. Fax: +1 919 962 0480.
E-mail address: lcqin@physics.unc.edu (L.-C. Qin).

0009-2614/$ - see front matter © 2004 Elsevier B.V. All rights reserved.
doi:10.1016/j.cplett.2004.11.004

we will also examine the effect on diffraction symmetry under two possible orientations of nanotubes with respect to the incident electron beam as encountered experimentally: (a) the nanotube is perpendicular to the incident electron beam; and (b) the nanotube axis is at a tilt angle β with respect to the diffraction plane that is perpendicular to the incident electron beam.

2. Theoretical considerations

A single-walled carbon nanotube can be formed by wrapping up a two-dimensional graphene sheet along a chosen tubule axis. In terms of crystallographic indices (u, v), a carbon nanotube can be defined by its perimeter vector $\vec{C}_h = u\vec{a} + v\vec{b}$ ($\vec{a}$ and $\vec{b}$ are the basis vectors of graphene lattice; they have the same magnitude $a_0 = 0.2451$ nm and an inter-angle 60°). Using the cylindrical coordinates (R,Φ, Z), the scattering amplitude (structure factor) on a layer line l can be expressed as follows [10]:

$$F_{uv} = (R, \Phi, l) = \sum_{n=-\infty}^{+\infty} \exp\left[in\left(\Phi + \frac{\pi}{2}\right)\right] J_n(\pi d R) \times \sum_j f \exp\left[i\left(-n\phi_j + \frac{2\pi l z_j}{c}\right)\right], \quad (1)$$

where f is the atomic scattering amplitude of carbon for electrons, d is the diameter of the carbon nanotube, c is the structural periodicity of the nanotube in the axial direction, J_n is the Bessel function of order n, and (d/2,ϕ_j,z_j) are the cylindrical coordinates of the positions of carbon atoms of the nanotube. Inserting the atomic positions for a carbon nanotube (u, v), the scattering amplitude (Eq. (1)) becomes

$$F_{uv}(R, \Phi, l) = \sum_{n,m} f \chi_{uv}(n, m) \gamma_{uv}(n, m) J_n(\pi d R) \times \exp\left[in\left(\Phi + \frac{\pi}{2}\right)\right], \quad (2)$$

where

$$\chi_{uv}(n, m) = 1 + \exp\left[2\pi i \frac{n + (2u + v)m}{3u}\right], \quad (3)$$

and

$$\gamma_{uv}(n, m) = \frac{1 - \exp[-2\pi i(n + mv)]}{1 - \exp[-2\pi i(n + mv)/u]} = \begin{cases} u & \text{if } (n + mv)/u = N, \\ 0 & \text{otherwise,} \end{cases} \quad (4)$$

in which n, m, and l are all integers that are governed by the following selection rule applied to carbon nanotube (u, v) [10]

$$l = \frac{(u + 2v)n + 2(u^2 + v^2 + uv)m}{uM} \quad (5)$$

with M being the maximum common divisor of integers ($u + 2v$) and ($2u + v$). Eqs. (4) and (5) constrain the values of n, the order of Bessel functions contributing to layer line l. The electron diffraction intensity from a single-walled carbon nanotube is only distributed on the layer lines that satisfy the selection rule expressed in Eq. (5), and the intensity distribution of layer line l is then given by

$$I_{uv}(R, \Phi, l) = |F_{uv}(R, \Phi, l)|^2. \quad (6)$$

Under the constraints governed by the selection rule, all the possible values of n for one chosen layer line l can be expressed as follows:

$$n = -n_0 - \frac{2P(u^2 + v^2 + uv)}{M}, \quad (7)$$

where P are integers that make n also an integer and n_0 defines the smallest non-negative integer for the chosen layer line l. On the other hand, since $(u^2 + v^2 + uv)/M$ is always an integer [14], from Eq. (7), we can obtain that, for any chosen layer line l, the evenness/oddity of all the orders n of contributing Bessel functions are the same as n_0. As an example, Fig. 1 shows schematically the diffraction geometry of the major layer lines on which the principal reflections of graphene reside as indicated by the apices of the graphene hexagons. If the helicity of the nanotube is α, as indicated schematically by the two twisted hexagons in the reciprocal space, we can derive from the geometry that l is equal to $(2u + v)/M$ for the layer line indicated by the dark arrows, which requires that n_0 be equal to $-v$ [15]. Thus, if v is even (odd), all the possible n along that layer line

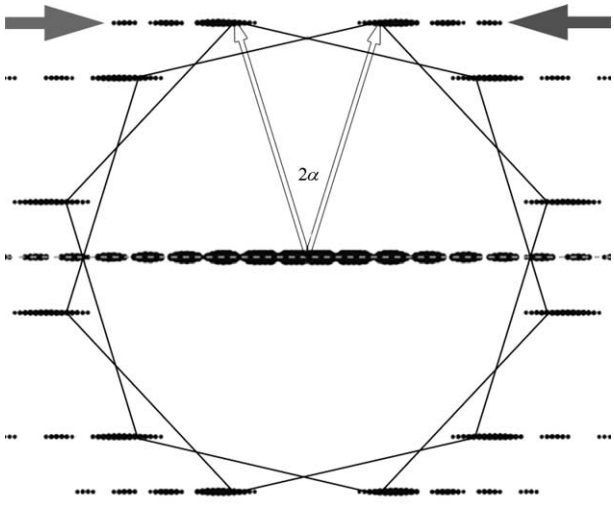

Fig. 1. Schematic electron diffraction pattern of a single-walled carbon nanotube with only the major layer lines. The helicity α of the nanotube is related to the relative twist of the two hexagons corresponding to the top and the bottom layer of the nanotube. From the geometry, the layer line number l (indicated by the arrows) is $(2u + v)/M$.

will be also even (odd). In addition, from Eq. (7) we can see that $2(u^2 + v^2 + uv)/M$ is usually a very large number. Since the magnitude of Bessel functions decreases significantly with the increase of their orders, the diffraction intensity on a particular layer line is essentially dominated by a single Bessel function of the lowest order $|n_0|$. For example, for single-walled carbon nanotube (14, 9) whose helicity is 23°, for the layer line l, $n_0 = -9$ and the next contributing Bessel function is $n = 797$. The magnitude of the first peak for $|J_9(x)|^2$ is more than 20 times of that for $|J_{797}(x)|^2$. Furthermore, the first peak position along the specified layer line for $(J_{797}(x)$ is 75 times larger than that for $J_9(x)$. Therefore, the diffraction intensity distribution on the layer line $l = 37$ for single-walled carbon nanotube (14, 9) is only modulated by $|J_9(x)|^2$ within the range of collection where significant experimental data are present in the reciprocal space.

3. Results and discussion

Electron diffraction patterns of single-walled carbon nanotubes are taken under two conditions: (i) normal incidence, i.e., the incident electron beam is perpendicular to the tubule axis, and (ii) inclined incidence, i.e., the incident electron beam is not perpendicular to the tubule axis. Since the electron diffraction intensity distributions are different under the above two conditions, their symmetry is discussed separately.

3.1. Normal incidence ($\beta = 0°$)

When the incident electron beam is perpendicular to the tubule axis, i.e., $\beta = 0°$ as shown in Fig. 2a and b, the tubule axis is in the diffraction plane that intersects the reciprocal space pattern of the nanotube. Under normal incidence, the dark line in Fig. 2c (intersection of the diffraction plane and the three-dimensional power spectrum of the carbon nanotube in the reciprocal space) should pass through the center of the concentric corona representing the intensity variations of a Bessel function. Along the dark line, since the orders of all contributing Bessel functions n have the same evenness/oddity, the intensity distribution (Eq. (2)) on dependence of Φ observes the following relationship

$$I(R, \Phi + \pi, l) = I(R, \Phi, l), \tag{8}$$

which is true for all the layer lines in the electron diffraction pattern. Eq. (8) demonstrates that the electron diffraction from a single-walled carbon nanotube has two-fold symmetry about the nanotube axis. Combining with the inversion symmetry $\bar{1}$ which is governed by the

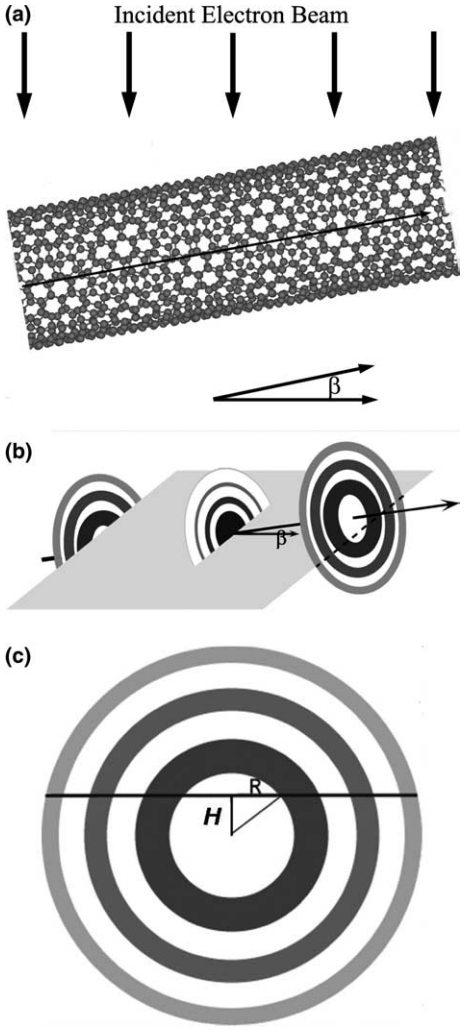

Fig. 2. (a) Schematic in real space showing the relative orientation when the electron beam is incident at a tilt angle β with respect to the diffraction plane (horizontal). (b) Schematic in reciprocal space illustrating the formation of electron diffraction pattern from a single-walled carbon nanotube. The power spectrum of a carbon nanotube (represented by three sets of coronae perpendicular to the tube axis) is intersected by the diffraction plane. The tilt angle β in (a) is reflected as the angle between the tube axis and the black arrow in the diffraction plane. The layer line spacings in the diffraction pattern are magnified by a factor of 1/cos β. (c) Diffraction coronae on the left viewed in the axial direction. The horizontal line indicates the intersection of the diffraction plane and the diffraction coronae with a distance $H = (l/c)\tan(\beta)$. When the tilt angle β is equal to zero, the intersection passes through the center of the coronae.

Friedel's law, the electron diffraction patterns of a single-walled carbon nanotube under normal incidence will therefore always have 2mm symmetry.

Fig. 3a shows a transmission electron microscope (TEM) image of a single-walled carbon nanotube. The two dark lines correspond to the projection of carbon atoms in the imaging plane, giving the diameter of this nanotube to be 1.5 ± 0.1 nm. An electron diffraction pattern of this nanotube is shown in Fig. 3b with the incident electron beam perpendicular to the tubule axis.

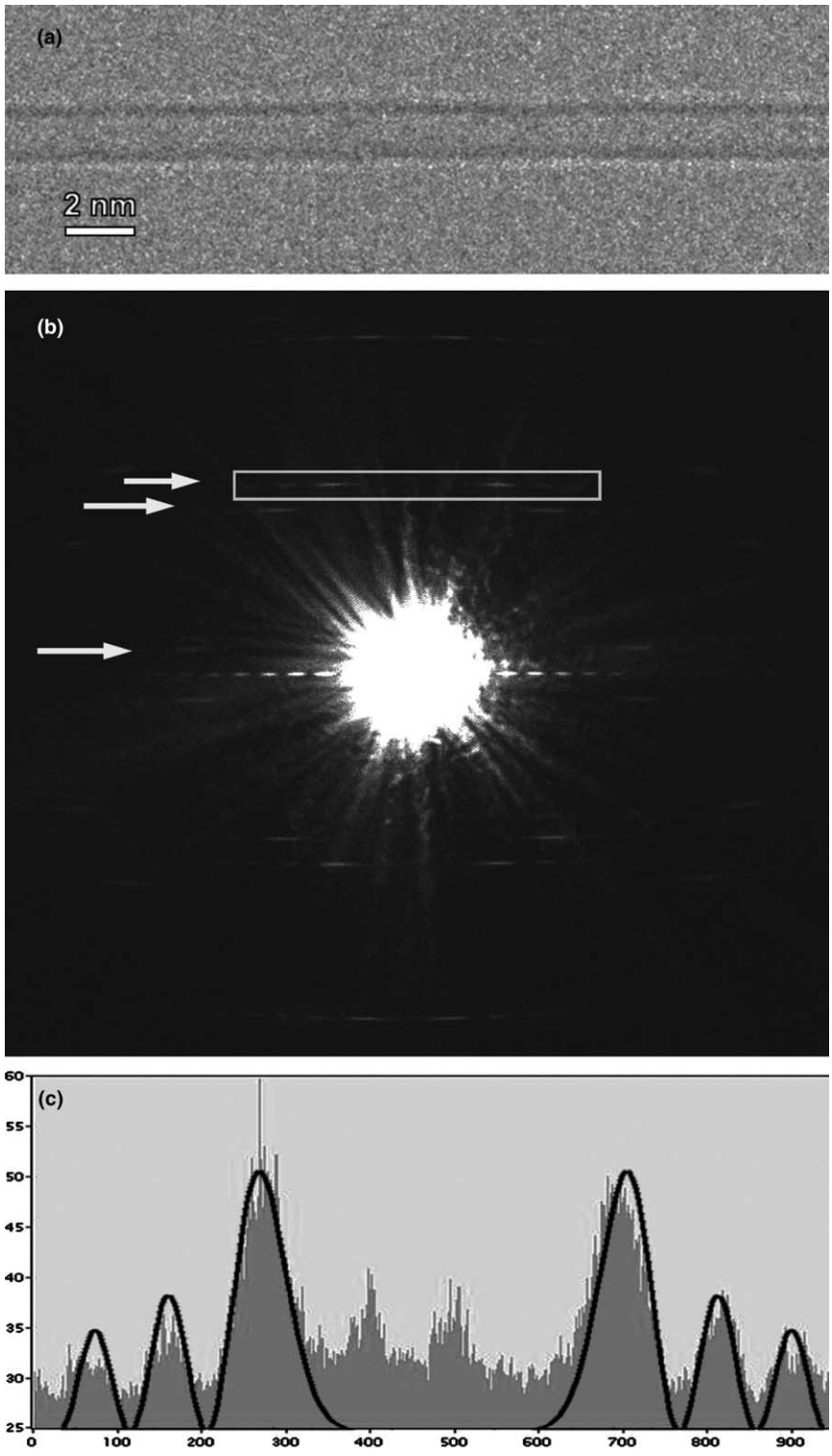

Fig. 3. (a) TEM image of a single-walled carbon nanotube of diameter $d = 1.5 \pm 0.1$ nm. (b) Electron diffraction pattern of the carbon nanotube. 13 layer lines are visible in the diffraction range of 10 $nm^{-1} \times 10$ nm^{-1}. The helicity of this nanotube is measured to be $23.0° \pm 0.1°$ from the three layer line spacings indicated by arrows. (c) Intensity profile of the enclosed region in (b). Solid line shows the calculated intensity profile. Mirror symmetry about the tube axis is observed in the experimental electron diffraction intensity profile, though the atomic structure of this nanotube lacks this symmetry.

In the diffraction range of 10 $nm^{-1} \times 10$ nm^{-1} as shown in Fig. 3b, we can observe 13 reflection layer lines. By measuring the layer line spacings between the layer lines indicated by the two upper arrows and the central layer line, the helicity of this nanotube is determined: $\alpha = 23.0° \pm 0.1°$. Combining the measured diameter

and helicity, the crystallographic indices of this nanotube are found to be (14, 9) – it is a semiconducting nanotube. The intensity profile on the layer line in the enclosed region in Fig. 3b is shown in Fig. 3c, which shows clearly mirror symmetry about the tubule axis. The simulated intensity profile is also plotted (solid line) on the same figure for comparison. The whole electron diffraction pattern has 2mm symmetry.

3.2. Inclined incidence $\beta \neq 0°$

When the incident electron beam is not perpendicular to the tubule axis, i.e., $\beta \neq 0°$, the diffraction plane does not pass through the tubule axis in the reciprocal space of the carbon nanotube, although it still passes through the center of the central diffraction coronae [16,17]. The points of intersection with the diffuse coronae representing the intensity variations of a Bessel function, depend on the tilt angle β and the positions of the layer line planes in the reciprocal space, as shown schematically in Fig. 2b. Fig. 2c shows the side view of the layer line plane on the left of the origin and the dark line indicates the intersection of the diffraction plane and the power spectrum of the nanotube in the reciprocal space. In the electron diffraction pattern under inclined incidence, the diffraction intensity on layer line l is modulated by Bessel functions of the same orders n as those under normal incidence as shown in Fig. 2c. However, the scattering amplitude measured on the diffraction plane is

$$F_{uv}(R,\Phi,l) = \sum_{n,m} f\chi_{uv}(n,m)\gamma_{uv}(n,m)J_n\left(\pi d\sqrt{R^2+\left(\frac{l\tan\beta}{c}\right)^2}\right) \times \exp\left[in\left(\Phi+\frac{\pi}{2}\right)\right]. \quad (9)$$

As discussed before, the evenness/oddity of n is the same for all allowed values. The electron diffraction intensity therefore also satisfies the following equation for all layer lines:

$$I(R,\pi+\Phi,l) = I(R,\Phi,l). \quad (10)$$

The whole electron diffraction pattern of a single-walled carbon nanotube under inclined incidence also has 2mm symmetry.

Fig. 4 shows the simulated electron diffraction patterns of the single-walled carbon nanotube (14, 9) under different incident directions. When the incident electron beam is perpendicular to the tubule axis ($\beta = 0°$), the simulated electron diffraction intensity shows 2mm symmetry, as shown in Fig. 4a. When the tilting angle β is increased from 0° to 10° (Fig. 4b), the split diffraction

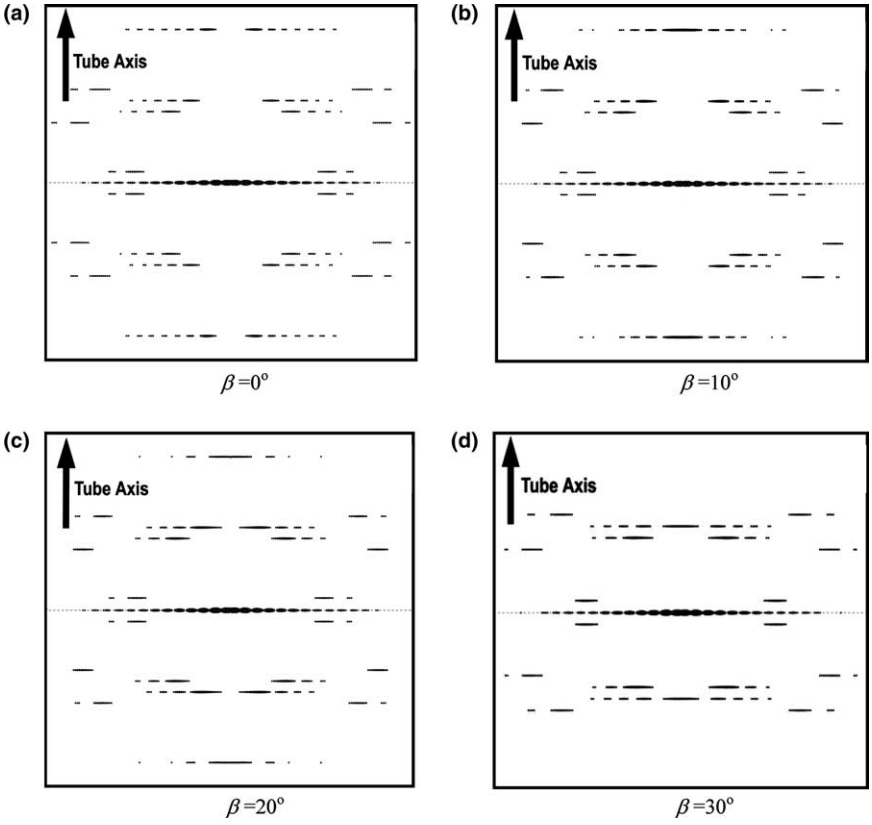

Fig. 4. Simulated electron diffraction patterns of single-walled carbon nanotube (14, 9) at various tilt angles. (a) $\beta = 0°$, (b) $\beta = 10°$; (c) $\beta = 20°$; (d) $\beta = 30°$. Though the intensity distribution varies as the tilt angle changes, the whole diffraction pattern always has 2 mm symmetry.

intensities across the tubule axis on the layer lines move towards the tubule axis. At the same time, the layer line spacings increase by a factor of 1.015 (=1/cos 10°). As we continue to increase the tilting angle β to 20°, shown in Fig. 4c, the split diffraction intensities on the layer line move closer toward the tubule axis and eventually merge into one at the tilt angle $\beta_c = \theta = \tan^{-1}[\frac{u_n}{n}\tan(\alpha)] = 26.8°$, where $n = 9$ and $u_n = 10.7$, the value at which Bessel function $J_9(u)$ assumes its first peak [3]. At $\beta = 30°$, which is larger than the critical tilt angle β_c, the diffraction plane will not intersect with the first ring of the coronae as illustrated in Fig. 2c and no significant intensity is observed at the position corresponding to the first major layer line as shown in Fig. 4d. During the process of tilting, the 2mm symmetry of the whole electron diffraction patterns is retained.

We would like to point out that, in general, the atomic structure of a single-walled carbon nanotube does not have mirror symmetry perpendicular to the tubule axis when discrete atoms are located at continuous helices around the nanotube, even though the projection of continuous helices does have mirror symmetry about the tubule axis.

4. Conclusions

Electron diffraction patterns of single-walled carbon nanotubes will always have 2mm symmetry no matter if they are placed at normal incidence and inclined incidence with respect to the electron beam. The 2mm symmetry is originated from the fact that the diffraction intensity distribution on any layer line is modulated by Bessel functions of all even or all odd orders governed by the selection rules. In addition, on any given layer line, the reflection intensity is dominated by contribution that can be described by a Bessel function of a particular order. Higher order terms are negligible.

References

[1] S. Iijima, Nature (London) 354 (1991) 56.
[2] S. Iijima, T. Ichihashi, Nature (London) 363 (1993) 603.
[3] L.-C. Qin, T. Ichihashi, S. Iijima, Ultramicroscopy 67 (1997) 181.
[4] L.-C. Qin, S. Iijima, H. Kitaura, Y. Maniwa, S. Suzuki, Y. Achiba, Chem. Phys. Lett. 268 (1997) 101.
[5] J.M. Cowley, P. Nikolaev, A. Thess, R.E. Smalley, Chem. Phys. Lett. 265 (1997) 379.
[6] J.-F. Colomer, L. Henrard, P. Lambin, G. Van Tendeloo, Euro. Phys. J. B 27 (2002) 111.
[7] M. Kociak, K. Suenaga, K. Hirahara, Y. Saito, T. Nakahira, S. Iijima, Phys. Rev. Lett. 89 (2002) 155501.
[8] M. Gao, J.M. Zuo, R.D. Twesten, I. Petrov, L.A. Nagahara, R. Zhang, Appl. Phys. Lett. 82 (2003) 2703.
[9] J.M. Zuo, I. Vartanyants, M. Gao, R. Zhang, L.A. Nagahara, Science 300 (2003) 1419.
[10] L.-C. Qin, J. Mater. Res. 9 (1994) 2450.
[11] A.A. Lucas, V. Bruyninckx, P. Lambin, Europhys. Lett. 35 (1996) 355.
[12] S. Amelinckx, A.A. Lucas, P. Lambin, Rep. Prog. Phys. 62 (1999) 1471.
[13] Z. Liu, L.-C. Qin, to be published.
[14] R. Saito, G. Dresselhaus, M.S. Dresselhaus, Physics Properties of Carbon Nanotubes, Imperial College Press, London, 1998.
[15] L.-C. Qin, Chem. Phys. Lett. 298 (1998) 28.
[16] X.B. Zhang, S. Amelinckx, Carbon 32 (1994) 1537.
[17] D. Bernaerts, M. Op De Beeck, S. Amelinckx, J. Van Landuyt, G. Van Tendeloo, Phil. Mag. A 74 (1996) 723.